MOMENTUM TRANSFER BY HYPERVELOCITY IMPACT: TARGET SHAPE AND STRUCTURE EFFECTS. M. Bruck Syal[1], J. M. Owen[1], and P. L. Miller[1], [1]Lawrence Livermore National Laboratory, Livermore, CA 94551 (syal1@llnl.gov)

Introduction: Asteroids found to pose a risk to Earth may be deflected off of an Earth-impacting orbit if detected and acted upon with suitable warning time [1,2]. Momentum transfer by hypervelocity impact represents a relatively simple method for accomplishing such deflections, yet the efficacy remains untested. The Asteroid Impact and Deflection Assessment (AIDA) mission will provide the first demonstration of the kinetic impactor concept for asteroid deflection, including a measurement of the total delivered momentum [3]. The properties of AIDA's target, the ~150-m secondary in the Didymos binary system, are not well-constrained. In the event of an actual asteroid threat, the issue of unconstrained physical properties (e.g., total mass, density, porosity, strength, rotational state, shape, and internal structure) is likely to arise as well. These details are available only for a handful of asteroids – those that have been well-characterized by prior spacecraft encounters or multiple radar observations.

In the absence of detailed information on a target asteroid, numerical studies can help quantify uncertainty in the body's response by exploring a range of initial conditions. Recent work focuses on the roles of equation of state, strength, porosity, and rotation on affecting the final outcome of kinetic impact deflection [4]. Here we examine how asteroid shape and structure affect momentum transfer in hypervelocity cratering events. While asteroid topography introduces natural variation in the impactor's incidence angle with the surface, oblique impacts will also be caused by targeting variabilities. These "off-axis" impacts alter the asteroid's rotational state, in addition to directing crater ejecta momentum along less-than-optimal trajectories. Crater ejecta that is above escape velocity contributes to the total momentum delivered to the asteroid; the magnitude of this additive effect is described by the quantity β:

$$\Delta\hat{p} = m_i\hat{v}_i + m_{ej}\hat{v}_{ej} = \beta m_i\hat{v}_i$$

where the "i" and "ej" indices indicate quantities describing the impactor and ejecta, respectively. Hence, when the ejecta momentum vector is not directed anti-parallel to the direction of intended deflection, the total impulse is decreased. The numerical treatment of shape effects described here complements recent analytical work on the problem [5].

We also examine the effects of rubble-pile-type internal structures on hypervelocity impacts into asteroids. While the low bulk densities of asteroids [6] may be partly explained by microporosity, macroporous structures, including larger voids between boulders, are also likely to be present and can affect shock propagation during impacts [7,8].

Numerical Methods: Three-dimensional simulations are carried out in Spheral [9,10], an open source, Adaptive Smooth Particle Hydrodynamics (ASPH) code. Key features of the code, including accurate modeling of anisotropic strain fields through adaptive node sampling, benchmarked damage models, self-gravity, an array of built-in equations of state and constitutive models, and user-extendibility to new physics packages, make Spheral well-suited for simulating impulsive asteroid mitigation scenarios [11,12].

We use the ANEOS equation of state for SiO_2 [13,14] to represent target asteroids, incorporate microporosity using a strain-alpha model [15], and use pressure-dependent strength [16]. Damage is calculated using a tensor generalization of the Grady-Kipp fracture model for SPH codes [17]. Standard impactors are represented by aluminum spheres. Between 10^6 and 10^7 ASPH particles were used in each simulation.

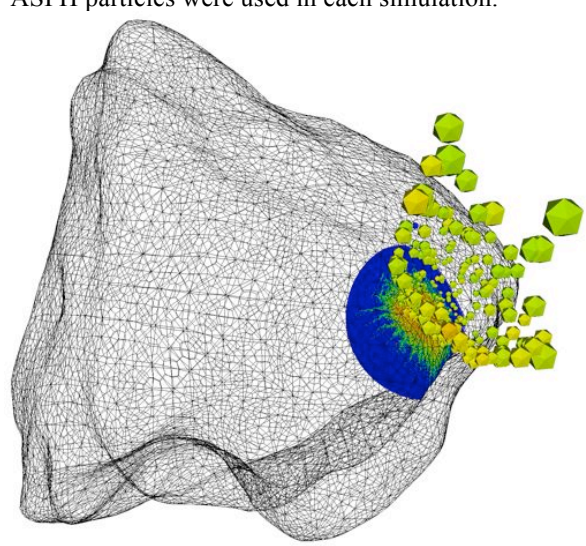

Fig. 1. Trace of the damage tensor is plotted at 0.074 seconds after a 10,000-kg mass impacts asteroid Golevka at 10 km/s along the x principal axis. Only the colored portion of the asteroid is modeled. The momentum vector of the the crater ejecta is directed at 26 degrees from the impactor trajectory, consistent with analytical models for the process [5].

Results: Asteroid Golevka serves as an interesting test case for shape effects, due to its unusual topography (including large concave regions, see Fig. 1) and its size (~500 m) [18], which places it near the upper limit of what a kinetic impactor could handle with decades of warning time [1]. Impacts were modeled along

the asteroid's three principal axes, in both directions, to separate the effects of local topography from offset impact effects. In order to model the impact at high spatial resolution, only the region extending 80 m from the impact site was included in the domain, as seen in the v_x = - 10 km/s case pictured in Fig. 1, 2.

The time evolution of the angle between the ejecta's momentum vector and the impactor's trajectory is plotted for each of the six principal axes cases in Fig. 3. The final values for these angles are consistent with the analytical model for shape effects described in [5], in which local surface normal determines the direction of the ejecta momentum vector.

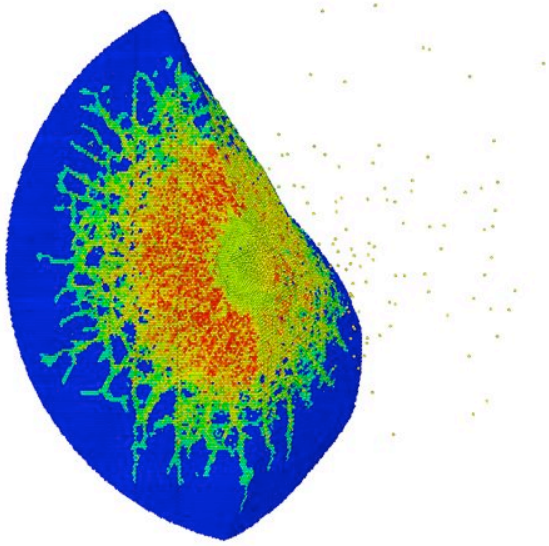

Fig. 2. Cross-sectional view of damge trace, from same result as shown in Figure 1 (v_x = - 10 km/s). At this time, the value for β has converged to 2.33, which corresponds to a very subtle velocity change to Golevka: Δv = 1 mm/s.

Implications: Uncertainties in asteroid shape and structure prior to impulsive deflection attempts can introduce significant perturbations to the final change in velocity. Even for the small number of asteroids with well-characterized shapes, the geometry of the impact may remain uncertain, due to impact timing and the asteroid's rotational state. Most impacts will likely diverge substantially from the idealized case of a normal impact through the asteroid's center of mass. Momentum transfer decreases as impacts become increasingly oblique; targeting errors of just tens of meters can produce a glancing impact for a 100-m-diameter asteroid. This asteroid size is large enough to cause regional devastation on Earth, meriting analysis of deflection options; however, predictions of delta-v for kinetic missions should incorporate possible degradation of the momentum impulse from shape and structure, including offset impact effects.

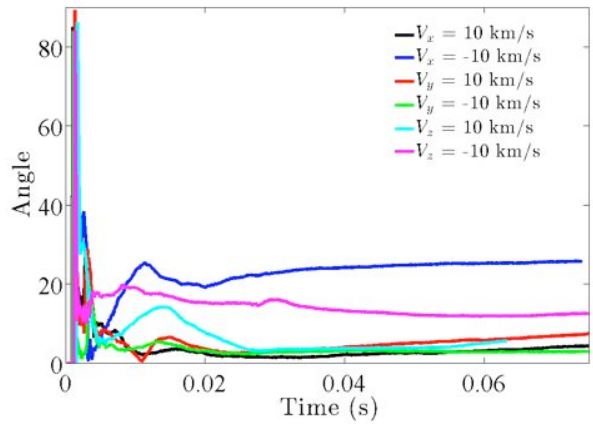

Fig. 3. Time evolution of angle between ejecta momentum vector and impactor trajectory for impacts along six principal axis directions at asteroid Golevka. Momentum vector diverges as much as 26 degrees from the intended direction of push, due to Golevka's irregular shape. Final push direction is determined by local surface normal, which controls the ejecta momentum direction [5].

References:

[1] Dearborn, D.S.P. & Miller, P.L., 2014. In *Handbook of Cosmic Hazards & Planetary Defense*, Springer. [2] Reinhardt, J. C. et al. 2014. *PSAM* **12**. [3] Cheng, A. et al. 2015. *Acta Astronaut.* **115**, 262–269. [4] Bruck Syal, M. et al. 2016. *Icarus*, In Press. [5] Scheeres, D. et al. 2015 *IEEE Aerospace Conference Contributions*, Big Sky, MT. [6] Britt, D.T. et al. 2002. In *Asteroids III,* U. Arizona Press. [7] Asphaug et al. 1998. *Nature* **393**, 437-440. [8] Asphaug et al. 2002. In *Asteroids III,* U. Arizona Press. [9] Owen, J. M. et al. 1998. *Astrophys. J. Suppl. S.* **116**, 155–209. [10] Owen, J. M. 2010. 5th International SPHERIC SPH Workshop. [11] Owen, J. M. 2014. *Int. J. Numer. Meth. Fl.* **75**, 749-774. [12] Owen, J. M. 2015. *Procedia Engineering* **103**, 466–474. [13] Thompson, S. and Lauson, H. 1972. SC-RR-710714, Sandia Natl. Lab., Albuquerque, NM. [14] Melosh, H.J. 2007. *Meteorit. Planet. Sci.* **42**, 2079– 2098. [15] Wünnemann, K. et al. 2006. *Icarus* **180**, 514–527. [16] Collins, G.S. et al. 2004. *Meteorit. Planet. Sci.* **39**, 217–231. [17] Benz, W. & Asphaug, E. 1995. *Comput. Phys. Commun.* **87**, 253–265. [18] Hudson, R.S. et al. 2000. *Icarus* **148**, 37-51.

This work was performed under the auspices of the U.S. Department of Energy by Lawrence Livermore National Laboratory under Contract DE-AC52-07NA27344. LLNL-ABS- 680772